Details of a Shock-Separated Turbulent Boundary Layer at a Compression Corner

Gary S. Settles,* Irwin E. Vas,† and Seymour M. Bogdonoff‡
Princeton University, Princeton, N.J.

An experimental study is described in which detailed mean-flow measurements are made in a shock wave-boundary-layer interaction. The interaction is produced by a 24° compression corner mounted on the wall of the Princeton University high Reynolds number wind tunnel. The experiments are performed at Mach 2.85 and $Re_{\delta 0} = 1.33$ million. A detailed mapping of the flowfield is presented, including separated region shape and location and velocity profiles. Results indicate a relatively straight zero-velocity line, a persistent downstream normal pressure gradient, and reverse velocities up to 16% of u_∞.

Nomenclature

A = area, ft^2
C_f = skin friction coefficient $\equiv \tau_w/(\rho_\infty u_\infty{}^2/2)$
M = Mach number
N = exponent in the velocity profile power-law formula: $(u/u_e) = (y/\delta)^{1/N}$
p = pressure, psia
p_{t2} = pitot pressure, psia
Re = freestream unit Reynolds number, $\rho_\infty u_\infty/\mu_\infty$, in.$^{-1}$
T = temperature, °R
T_t = tunnel stagnation temperature, °R
T_{t2} = total temperature measured by probe, °R
u = mean streamwise velocity, fps
u_{e0} = incoming freestream velocity = 1875 fps
U^+ = u/u_τ, wall-wake velocity coordinate
u_τ = friction velocity
x = distance along model surface measured from corner, in.; also distance along tunnel centerline from nozzle throat, in.
y, Y = distance normal to model surface, in.
Y^+ = $u_\tau y/\nu$, wall-wake Reynolds number
α = ramp angle, degrees
δ = boundary-layer thickness, in.
δ_0 = incoming boundary-layer thickness = 0.83 in.
δ^* = boundary-layer displacement thickness, in.

$$\equiv \int_0^\delta \left(1 - \frac{\rho u}{\rho_\infty u_\infty}\right) dy$$

θ = boundary-layer momentum thickness, in.,

$$\equiv \int_0^\delta \frac{\rho u}{\rho_\infty u_\infty}\left(1 - \frac{u}{u_\infty}\right) dy$$

μ = viscosity coefficient
ν = kinematic viscosity, μ/ρ
ψ = stream function, $\equiv \int_0^Y \rho u\, dy$
ρ = density
τ = shear stress, lb/in.^{2}

Subscripts

t = stagnation conditions
∞ = freestream conditions
e = boundary-layer edge condition
0 = undisturbed flow condition at corner location
c = corner condition
max = maximum
rev = reverse
s = station
w = wall condition
div = dividing streamline
x = based on x
δ = based on δ

Received Jan. 20, 1976; presented as Paper 76-164 at the AIAA 14th Aerospace Sciences Meeting, Washington, D.C., Jan. 26-28, 1976; revision received Sept. 22, 1976. This work was supported by Air Force Office of Aerospace Research, Aerospace Research Lab., Contract No. F33615-73-C-4156 and Air Force Office of Scientific Research, Contract F44620-75-C-0080.

Index categories: Boundary Layers and Convective Heat Transfer—Turbulent; Supersonic, and Hypersonic Flow; Shock Waves and Detonations.

*Consultant; Research Scientist at Princeton Combustion Laboratories/Flow Research, Inc., Princeton, N.J. Member AIAA.

†Senior Research Engineer and Lecturer, Gas Dynamics Laboratory. Associate Fellow AIAA.

‡Professor and Chairman, Dept. of Aerospace and Mechanical Sciences. Fellow AIAA.

Introduction

ONE of the most interesting, important, and difficult problems of fluid mechanics is the interaction of a shock wave and a turbulent boundary layer resulting in flow separation. The problem is not a new one; it has provoked many significant studies in the past (e.g., Refs. 1 and 2). Nevertheless, even two-dimensional examples of this complex viscous-inviscid fluid interaction are not well understood.

The relative roles of experiment and numerical computation in investigating such flows are presently subject to much controversy.[3,4] While the experimental difficulties of the shock-turbulent boundary-layer interaction problem are formidable, its theoretical difficulties are even more so. Still, modern techniques of numerical computation and the high-speed computer may eventually yield routine solutions of the problem. If such solutions are ever to occur, their development will depend heavily upon careful and detailed experiments for guidance.

Thus there is much justification for the further experimental study of shock-boundary-layer interactions, both to provide a guide for computations and to further the knowledge of the mechanism and behavior of these interactions. For both purposes, attention must be directed toward the careful study of the interaction details, which have been overlooked in many past studies.

The present authors have shown[5,6] that attention to detail and redundant measurements over a wide range of Reynolds numbers leads to a considerably altered view of the incipient separation aspect of shock-boundary-layer interaction. A similar philosophy is applied to a separated flowfield in the present study. The adiabatic interaction of a Mach 2.85

freestream and turbulent boundary layer with the shock-wave system produced by a 24° compression corner was experimentally studied and is reported here. Detailed profile measurements were made in order to piece together an experimental model (or map) of the entire interaction region. Due to space limitations, only the major results of the study are presented here. For complete details, the reader should consult Ref. 7.

Experimental Procedures

The Princeton 8 × 8 Wind Tunnel

Tests were carried out in the Princeton University high Reynolds number 8 × 8-in. supersonic blowdown tunnel.[8] The test model was mounted on the wind tunnel wall 46 in. downstream of the nozzle exit, at which location the freestream flow is uniform at a Mach number of 2.85. Tests were conducted at a stagnation temperature of 472°R (±2%). The corresponding freestream unit Reynolds number is 1.6×10^6/in. Measurements are referenced to the undisturbed incoming flowfield parameters: $\delta_0 = 0.83$ in., $u_{e0} = 1875$ fps.

24° Compression Ramp Model

A solid brass test model incorporating a flat wall segment, a 24° compression corner, and a 6-in.-long ramp face was used. The width of the compression ramp (6 in.) allowed a 1-in. gap on either side for the passage of the tunnel sidewall boundary layers. Aerodynamic fences (see section on two dimensionality, and Ref. 6) were attached to the ramp sides to further isolate the compression corner from the sidewall boundary-layer influences. The model incorporated 88 surface taps for longitudinal and transverse surface pressure measurements.

Survey Probes

Pitot pressure, static pressure, total temperature, reverse pitot, and Preston tube probes were used. The pitot probes had 0.007-in. flat tips with 0.003-in. orifices. The reverse pitot tip was kinked to prevent its wake from returning in the same plane to interfere with its reading. The Preston tube had an outside diameter of 0.62 in. and an inner-to-outer diameter ratio of 0.6. A fine-wire total-temperature probe similar to the one described by Vas[9] was used. Static pressures were measured by a small, conventional needle-type probe having a tube diameter of 0.032 in. and a 15° conical tip.

Flow Visualization Techniques

The shock boundary-layer interaction flowfield was observed and photographed by means of the conventional shadowgraph and Schlieren techniques. Surface flow patterns over the 24° ramp model were obtained using the kerosene-graphite technique described fully in Appendix B of Ref. 6.

Probe Interference

There clearly exists a possibility that the survey probes used might affect the flow quantities which they are intended to measure. Accordingly, the surface pressures, surface flow pattern, and shadowgraph pattern were closely monitored during several probe surveys. Even when the probe tip was allowed to touch the model surface inside the separated region, only negligible changes were noticed in these measurements. Shadowgrams indicated that any strong shock waves created by the probes intersected the model well downstream of the compression corner, where they had little effect. The static pressure probe, when in contact with the model, read pressures very near the undisturbed wall-tap values. The weight of this evidence suggests that probe interference was not a significant factor in these tests. This conclusion agrees with the observations of Behrens[10] in a similar experiment.

Flowfield Steadiness

A special test series involving sequences of microsecond spark shadowgrams and continuous-light photographs was undertaken to evaluate flowfield steadiness. Based on this evidence, no large fluctuations of the interaction size and shape were noticed. Minor motions and ripples of the flow patterns were observed, but these amounted to 1/10th of δ_0 or less.

Data Reduction

Measured profiles of p, p_{t_2}, and T_{t_2} were combined to yield mean streamwise Mach number and velocity profiles. Small corrections were applied to the p and T_{t_2} data; the p_{t_2} data were uncorrected. The mean accuracy of the Mach number profiles thus derived is believed to be approximately ±3%. The accuracy of the u-velocity profiles is estimated at ±5%.

Results and Discussion

Incoming Boundary Layer

The complete family of 8 × 8 tunnel wall boundary-layer profiles is discussed in Ref. 6. One member of that family, the profile upstream of the present 24° ramp interaction, is shown in Fig. 1. The profile is mapped into incompressible coordinates via the Van Driest II transformation,[11] and is shown in the standard semilogarithmic U^+ vs Y^+ form. Also shown for comparison is the combined wall-wake law of Coles,[12] with which the data points are in good agreement. The thickness parameters of the profiles shown in Fig. 1 are $\delta_0 = 0.83$ in., $\delta_0^* = 0.237$ in., and $\theta_0 = 0.045$ in. It was found in Ref. 6 that the entire family of tunnel wall profiles, including the present one, are fully turbulent equilibrium boundary-layer profiles.

Surface Pressure Distribution

The measured surface static pressure distribution on the test model is shown in Fig. 2. The locations of separation and reattachment as determined from surface flow patterns are indicated in the figure. The presence of a separated region is clearly indicated by a "kink" in the pressure distribution.

The overall pressure rise does not quite reach the inviscid oblique-shock value of $p/p_0 = 4.5$ at the last surface tap location. However, the ramp face is longer than the critical value ($6\delta_0$) necessary to approximate infinite ramp length conditions according to the strong interaction analysis of Hunter and Reeves.[13] Experiments involving lengthing the ramp face produced no changes in the flowfield properties or the surface pressure distribution. The repeatability of the distribution shown in Fig. 2 is within ±2%.

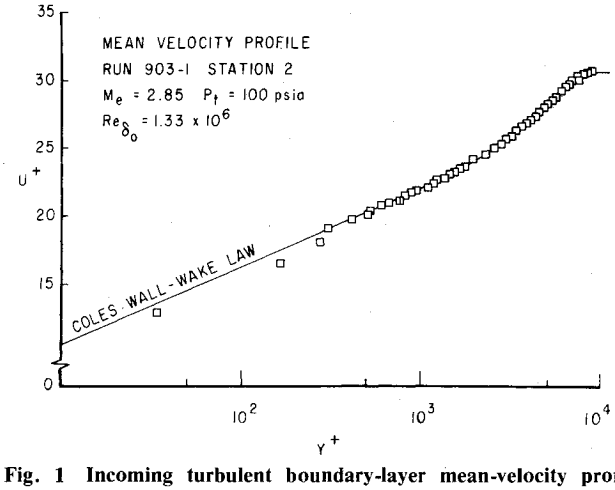

Fig. 1 Incoming turbulent boundary-layer mean-velocity profile compared with Coles wall-wake law.

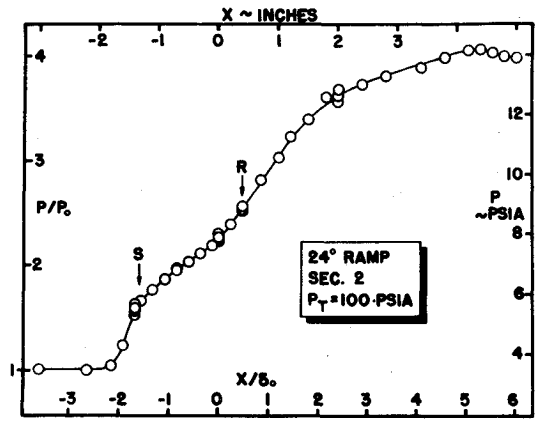

Fig. 2 Surface pressure distribution on the 24° compression corner model.

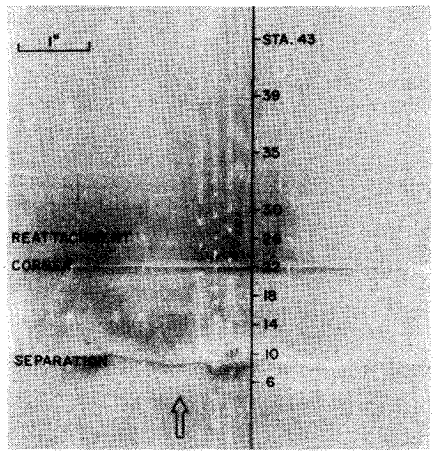

Fig. 3 Kerosene-graphite surface flow pattern on the 24° compression corner model.

Surface Flow Pattern

The kerosene-graphite surface flow pattern is shown in Fig. 3. Freestream flow is shown from bottom to top in the figure. The separation line, compression corner, and reattachment line locations are indicated. Since the kerosene-graphite technique[6] leaves an extremely thin, dry trace on the model, separation and reattachment locations are believed to be accurately represented. Also, these locations agree with those determined by pitot and Preston tube measurements.

The vertical line in Fig. 3 represents the probe survey plane. Some of the survey stations are indicated along this line. The sides of the figure correspond to the edges of the ramp, where the aerodynamic fences were attached.

Qualitative indications of the surface shear stress magnitudes and directions are given by the trails left by surface pressure taps in Fig. 3. These trails indicate reverse flow between stations 10 and 26, and forward flow elsewhere. No trails are left by taps at separation and reattachment, where the surface shear is zero.

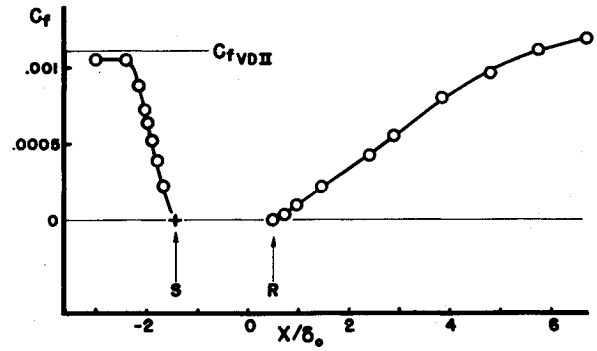

Fig. 4 Preston tube skin friction measurements along the shock boundary-layer interaction.

Two Dimensionality

The meaningfulness of the present study depends to a large extent on the essential two dimensionality of the 24° compression corner flowfield. This was ascertained early in the test program by several observations: a) only minor transverse surface pressure variations on the test model, b) only minor perturbations in an otherwise two-dimensional surface flow pattern, c) the interchangeability of different aerodynamic fences above a certain minimum size without affecting the flowfield, and d) agreement and consistency between the 24° data on separation length, pressure distribution, etc. and that of lower angle compression corner tests of known two dimensionality.[6,7]

These observations are, of course, no absolute proof of two dimensionality, but they appear to show that the existing three-dimensional perturbations of the flow are minor. No such essential two dimensionality was achieved without the use of the aerodynamic fences.

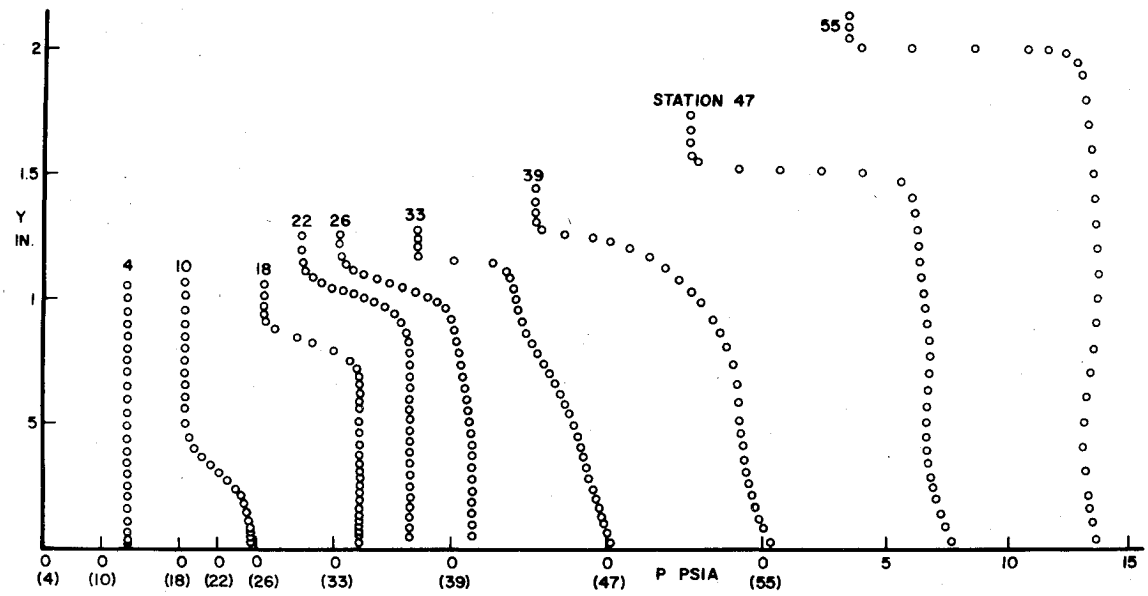

Fig. 5 Mach number contours in the shock boundary-layer interaction.

Skin Friction

A number of Preston tube readings were taken both upstream and downstream of the separated region. Due to the adverse pressure gradient it was necessary to use "effective" boundary-layer edge conditions (obtained from tunnel stagnation and local static pressures) in the data reduction.[14] Having done so, the present Preston tube skin friction results are presented in Fig. 4.

Figure 4 indicates that the skin friction coefficient drops rapidly from the incoming flat plate value to zero at the separation line, then rises more slowly from zero at reattachment to the vicinity of the flat plate value again near the ramp base. Good agreement is found between Preston tube results and the known C_f values at separation, at reattachment, and upstream of the interaction. Based on these facts and bearing in mind the drawbacks of the technique in an adverse pressure gradient, the Preston tube results of Fig. 4 are assigned a confidence level of about $\pm 10\%$.

Probe Survey Results

Large numbers of pitot pressure surveys were made, not only near the separated region but also spanning the interaction from the incoming boundary layer to the end of the ramp face. Surveys ahead of the compression corner were carried out along paths that tilted 5.5° forward with respect to the surface normal in order to align the probe with the average direction of shear flow behind the separation shock. Surveys at or downstream of the compression corner were carried out along paths normal to the ramp face. In each case, data were obtained outward from the model surface through the shock system and into the tunnel freestream flow. A total of about 50 pitot surveys was obtained.

The test program also included some 30 static pressure surveys at 21 different stations. A selection of these static pressure profiles is given in Fig. 5. The presence of the shock system generated by the 24° model is marked by an abrupt change in each static pressure profile, which becomes a near-discontinuity at the aft survey stations. Note that within the separated region (between stations 10 and 26) there is essentially no gradient of static pressure normal to the wall. Downstream of reattachment, however, a weak but noticeable normal pressure gradient persists to the last survey station. Recent additional experiments have shown similar behavior in another separated flowfield over a 20° compression corner, but no such lingering normal static pressure gradient in the attached flow downstream of an 8° compression corner.

Mach number profiles calculated from the pitot and static pressure measurements were used to construct the Mach number contour plot of Fig. 6. The shape of the sonic line is of particular interest. The sonic line lies very near the wall in the incoming boundary layer but breaks away from the wall at a 16° angle near the beginning of the interaction. This angle is greater than the 10° outer-flow turning indicated by the separation shock angle in the shadowgrams. The sonic line is slightly convex above the separated region, but turns upward near reattachment. The flow retardation downstream of reattachment is manifested by the sonic line remaining significantly displaced from the ramp face for a distance of $2\delta_0$ downstream of the compression corner. Waves in the supersonic part of the flowfield are generated and reflected from the sonic line, consequently its gradual curvature conforms to the fact that the reattachment compression fan is observed to be distributed rather than concentrated.

Forward and Reverse Pitot Surveys

A special series of 27 detailed forward and reverse pitot pressure surveys was conducted in the vicinity of the separated region. The series was aimed at locating the zero-velocity line, and the dividing streamline, and determining the reverse-flow velocity profiles.

Ten points on the line of zero u velocity were obtained at the crossing of forward and reverse surveys. The shape of the zero-velocity line is slightly concave near separation and slightly convex near reattachment, but otherwise quite straight. This is in line with the observation that strong normal and streamwise pressure gradients occur near separation and reattachment but not in between.

Reverse Velocity Results

The reverse pitot profiles, along with static pressure and total temperature measurements, were used to obtain the reverse velocity profiles in the separated region. These profiles are shown in Fig. 7. Maximum reverse velocities occur very near the surface. The peak reverse velocity is 16% of u_{e_0}, which corresponds to a reverse Mach number of 0.27.

Calculated mean-flow streamlines in the vicinity of the compression corner are depicted in Fig. 8, with the vertical coordinate stretched by a factor of two for clarity. Separation and reattachment points are indicated, and are connected by the $u=0$ line (dotted) and the dividing streamline (denoted by the zero value of the stream function ψ). The dividing streamline is commonly assumed to be straight, but is shown in this case to be quite convex. It encloses a single recirculating vortex whose core is directly above the compression corner. The "separation bubble" thus defined is shallow near the separation point but full and rounded near reattachment.

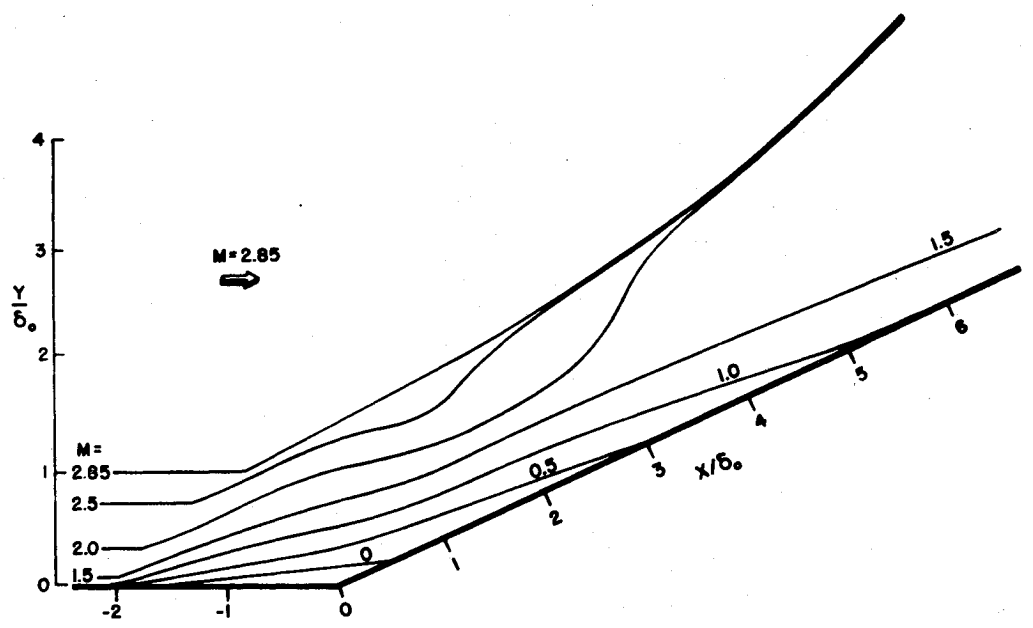

Fig. 6 Selected flowfield static pressure profiles.

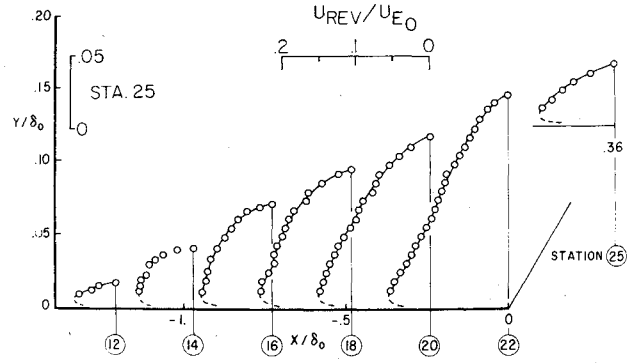

Fig. 7 Reverse mean-velocity profiles in the separated region.

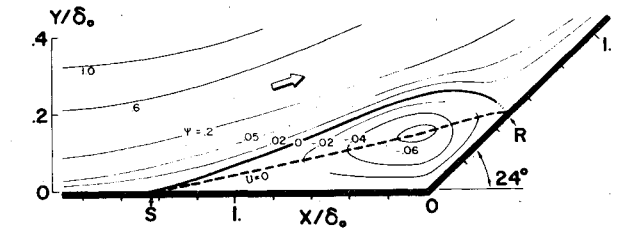

Fig. 8 Mean-flow streamlines in the vicinity of the 24° compression corner.

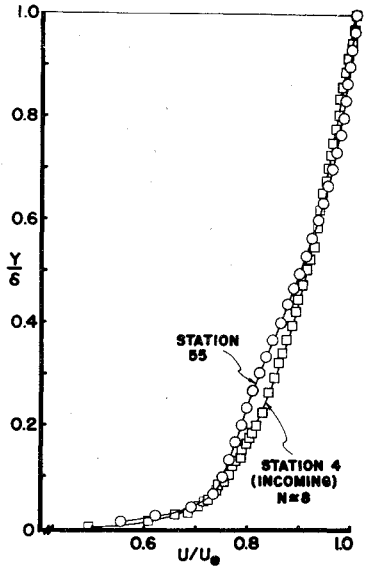

Fig. 10 Comparison of incoming and outgoing boundary-layer velocity profiles.

Forward Velocity Profiles

Nine mean-velocity profiles spanning the shock-boundary-layer interaction are shown in Fig. 9. These profiles are identified by station number and are spaced according to their station locations along the test model. The input profile is that of an equilibrium turbulent boundary layer, as previously discussed (Fig. 1). The profile at separation is identical to the input profile, except that it is retarded below $y/\delta_0 = 0.4$. At stations 18 and 22 are free shear layer profiles with reverse velocities near the wall. The reattachment profile (station 26) is highly retarded. Profiles downstream of reattachment show a gradual recovery, such that the station 55 profile is not obviously different from an equilibrium turbulent boundary-layer shape.

A direct comparison between incoming and outgoing velocity profiles is given in Fig. 10, where the two are in qualitative agreement. There is, however, a noticeable velocity defect in the station 55 profile in the range of $0.2 < y/\delta < 0.4$, indicating a strong wake component not yet relaxed from the effects of the interaction. Thus it is clear that, under the present test conditions, more than seven boundary-layer thicknesses downstream of the interaction are required for the complete recovery of the mean streamwise velocity profile.

Experimental Model

An experimental model or map of the 24° compression corner flowfield is shown in Fig. 11, based on the results of the present measurements. The influence of the 24° turn is felt two incoming boundary-layer thicknesses upstream of the compression corner, where an induced shock wave is formed. Separation occurs downstream of the induced shock. Locations of the zero-velocity line and the dividing streamline are shown. The external flow initially turns through a 10° angle, followed by the remaining 14° turn at reattachment. A system of compression waves is generated upon flow reattachment to the compression ramp surface. These waves eventually coalesce with the induced shock and strengthen it. The

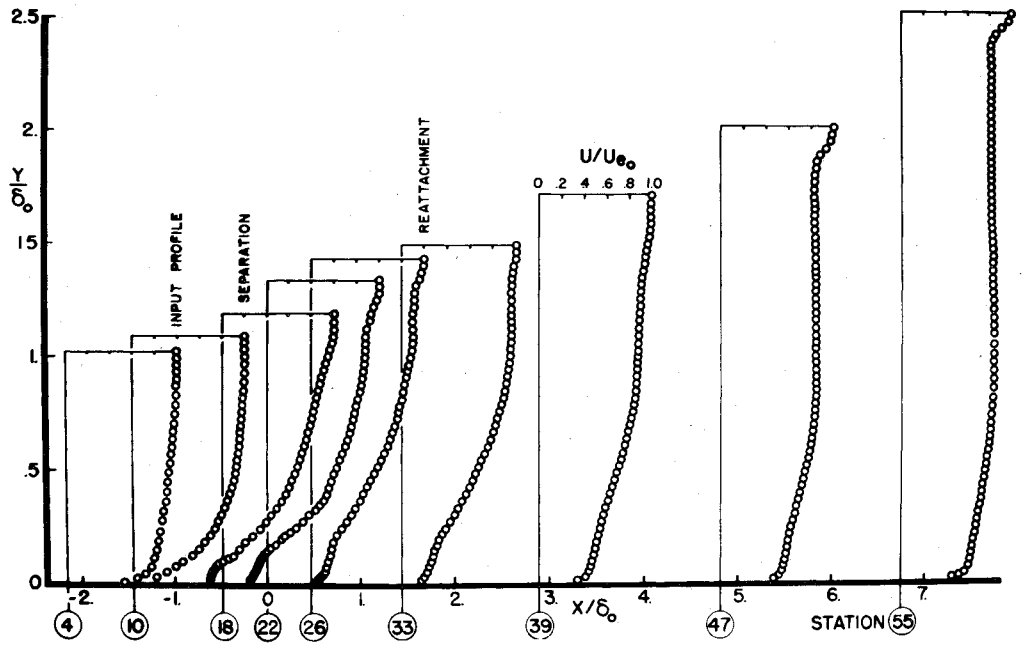

Fig. 9 Development of the mean streamwise velocity profiles through the shock boundary-layer interaction.

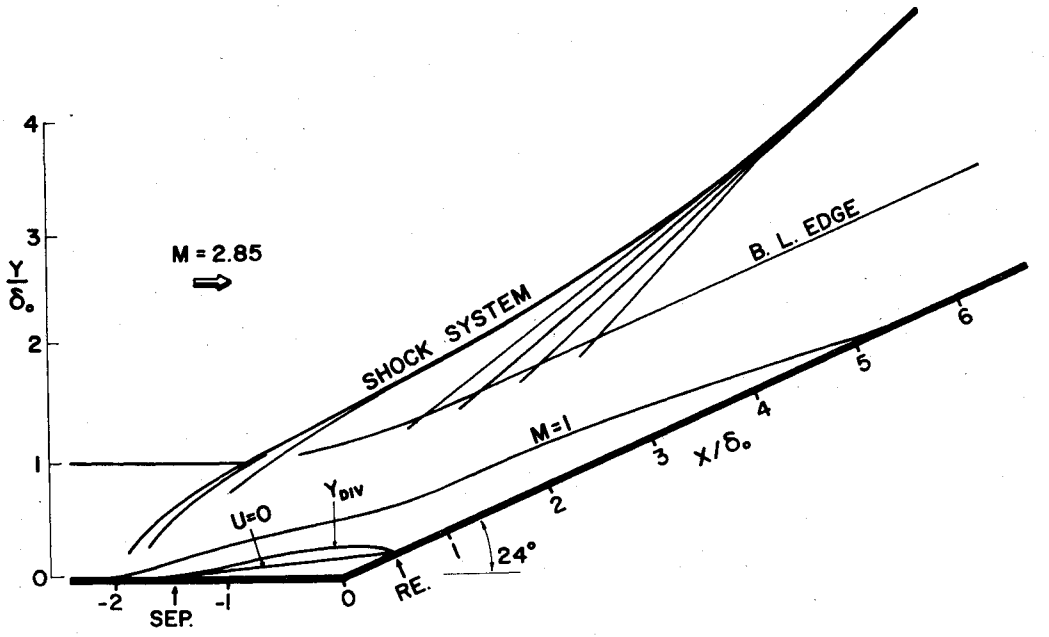

Fig. 11 Experimental model of the 24° compression corner flow field.

sonic line is considerably displaced from the surface throughout the interaction, but gradually reapproaches the surface well downstream of the compression corner.

Comparison With Prediction Techniques

The present study affords an opportunity to compare a shock-boundary-layer interaction in which most flow quantities have been measured or deduced (two notable exceptions are heat transfer and turbulent fluctuations) with the various semiempirical prediction methods, strong interaction theories, and Navier-Stokes solutions which are available.

A number of semiempirical prediction methods are available for shock-separated turbulent boundary-layer flows. They incorporate many assumptions, thus presenting very simplistic flowfield representations, but nonetheless may be of value.

Erdos and Pallone[15] and Popinski and Ehrlich[16] suggest correlations of the pressure coefficient at separation that disagree (by −13% and −20%, respectively) with the present measured value of 0.126. Reference 15 predicts a 9.5° flow turning after separation, agreeing with the 10° turn measured here, but their assumption of a straight dividing streamline is at variance with present results.

The analysis of Reshotko and Tucker[17] closely predicts the present momentum thickness change across separation, even though their boundary-layer momentum integral equation is jeopardized by the strong normal pressure gradient at separation.

Momentum- and displacement-thickness ratios across separation are underpredicted by as much as 30% by White[18] and Kessler and Page.[19] Batham's[20] reattachment correlation is found to underpredict the present reattachment pressure coefficient by 25%.

Pinckney[21] has proposed a simple one-dimensional model that predicts boundary-layer quantities throughout a shock wave interaction. His model somewhat overestimates the downstream recovery length of the interaction (11.5 δ_0 compared to present $\sim 9\delta_0$). Corresponding slight overpredictions in downstream-to-upstream thickness ratios are found: $\delta_{555}/\delta_0 = 1.2$ compared to measured 0.98, $\delta^*_{555}/\delta^*_0 = 1.33$ vs 0.76, and $\theta_{555}/\delta_0 = 1.7$ vs 1.18. Overall, however, Pinckney's prediction method is surprisingly accurate in view of its simplicity. In making the above comparisons, Pinckney's plots are slightly extrapolated and an equivalance is assumed between an incident-shock interaction with shock deflection angle β and a compression corner interaction with corner angle 2β.

A strong-interaction model of the separated shock turbulent boundary-layer interaction has been suggested by Reeves and associates.[13,22] These investigators display a wealth of experimental data comparing favorably with their model. The present results are also well-predicted in terms of separation bubble area ($A/\delta_0^2 = 0.23$ from theory and experiment) and separation length, although the surface pressure distributions do not compare well. It should also be mentioned that the Mach 3 incipient separation level and variation of this level with Reynolds number as predicted by Todisco and Reeves[22] is in good agreement with recent experiments reported by the present authors.[5,6]

The newest and most sophisticated theoretical approach to the present problem involves the numerical solution of the Navier-Stokes equations. Wilcox[23] has obtained such solutions using finite differences and the Saffman turbulence model. Fortunately, one of his solutions (26° compression corner, $M = 2.96$, $Re_{\delta_0} = 10^6$) approximates the present test conditions. Although the measured surface pressures and static pressures isobars are not well-predicted, the agreement between the shock wave, sonic line, and separated region shapes shown in Fig. 11 and those computed by Wilcox is surprisingly good.

Shang and Hankey[24] have performed a similar computation (25° compression corner, $M = 2.96$, $Re_x = 10^7$) with a less sophisticated, diffusive eddy viscosity turbulence model. Their computed velocity profiles through the interaction are in qualitative agreement both with those measured by Havener and Radley[25] and those shown in Fig. 9. A detailed comparison between this and other experimental results of the present authors and Navier-Stokes computational solutions by Horstman and Hung is given in Ref. 26.

Summary and Conclusions

In summary, detailed flowfield measurements have been made in the shock-separated turbulent boundary layer over an adiabatic 24° compression corner at Mach 2.85. This experiment was carried out at a length Reynolds number approaching 10^8, which typifies high-speed flight conditions. Analysis of the measurements results in a complete experimental map of the flowfield, as depicted in Fig. 11.

An induced shock wave originates approximately two boundary-layer thicknesses upstream of the corner, turning the outer flow through an initial 10° angle. A rounded separation bubble lies beneath the induced shock. The zero-velocity line within the bubble is nearly linear. A gradual flow

recompression takes place downstream of reattachment, with the sonic line of the flow remaining significantly displaced from the surface for a distance of five boundary-layer thicknesses.

A number of interesting facts arise from the present measurements. Static pressures in and above the separated region and well downstream of reattachment are observed to be relatively constant, whereas strong normal pressure gradients occur near the separation and reattachment points. A decaying normal pressure gradient in the outgoing boundary layer persists for five boundary-layer thicknesses distance downstream of the compression corner. Velocity profiles in this recovery region are highly retarded, and do not fully recover from the effects of the interaction by 7 δ_0 downstream.

High-resolution measurements and a relatively large boundary-layer thicknesses have led to profiles of forward and reverse velocities with a wealth of detail not usually presented in similar studies. Extensive checks indicate that the flowfield is approximately two dimensional and without serious mean-flow oscillations, and that the effects of probe interference are not significant.

A number of comparisons are made between the present results and available prediction methods and numerical computations. Measurements of heat transfer and turbulent fluctuation quantities are needed to complement the mean-flow results given here. An experimental program to that effect is now under way in the Princeton University Gas Dynamics Laboratory.

References

[1] Bogdonoff, S.M. and Kepler, C.E., "Separation of a Supersonic Turbulent Boundary Layer," *Journal of the Aeronautical Sciences,* Vol. 22, June 1955, pp. 414-424.

[2] Chapman, D. R., Kuehn, D. M., and Larson, H. K., "Investigation of Separated Flows in Supersonic Stream with Emphasis on the Effect of Transition," NACA Report 1356, 1958.

[3] Chapman, D. R., Mark, H., and Pirtle, M, W., "Computers vs. Wind Tunnels," *Aeronautics and Astronautics*, Vol. 13, April 1975, pp. 22-30.

[4] Roache, P. J., Letter to Editor on "Computers vs. Wind Tunnels," *Astronautics and Aeronautics*, Vol. 13, Sept. 1975, p. 4.

[5] Settles, G. S., Bogdonoff, S. M., and Vas, I. E., "Incipient Separation of a Supersonic Turbulent Boundary Layer at High Reynolds Numbers," *AIAA Journal*, Vol. 14, Jan. 1976, pp. 50-56.

[6] Settles, G. S., "An Experimental Study of Compressible Turbulent Boundary Layer Separation at High Reynolds Numbers," Ph.D. dissertation, Aerospace and Mechanical Sciences Dept., Princeton University, Princeton, N.J., Sept. 1975.

[7] Settles, G. S., Vas, I. E., and Bogdonoff, S. M., "Shock Wave-Turbulent Boundary Layer Interaction at a High Reynolds Number, Including Separation and Flowfield Measurements," AIAA Paper 76-164, Washington, D. C., Jan. 1976.

[8] Vas, I. E. and Bogdonoff, S. M., "A Preliminary Report on the Princeton University High Reynolds Number 8″ × 8″ Supersonic Tunnel," Internal Memorandum 39, Gas Dynamics Lab., Dept. of Aerospace and Mechanical Sciences, Princeton University, Princeton, N.J., 1971.

[9] Vas, I. E., "Flow Field Measurements Using a Total Temperature Probe at Hypersonic Speeds," *AIAA Journal*, Vol. 10, March 1972, pp. 317-323.

[10] Behrens, W., "Separation of a Supersonic Turbulent Boundary Layer by a Forward Facing Step," AIAA Paper 71-127, El Paso, Texas, 1971.

[11] Van Driest, E. R., "The Problem of Aerodynamic Heating," *Aerospace Engineering Review*, 1956, pp. 26-41.

[12] Coles, D. E., "The Turbulent Boundary Layer in a Compressible Fluid," Rand Corporation Rept. R-403-PR, 1962.

[13] Hunter, L. G., Jr. and Reeves, B. L., "Results of a Strong Interaction Wake-Like Model of Supersonic Separated and Reattaching Turbulent Flows," *AIAA Journal*, Vol. 9, April 1971, pp. 703-712.

[14] Oskam, B., Bogdonoff, S. M., and Vas, I. E., "Study of Three-Dimensional Flow Fields Generated by the Interaction of a Skewed Shock Wave with a Turbulent Boundary Layer," AFFDL-TR-75-21, Air Force Flight Dynamics Lab., Wright-Patterson AFB, Ohio, Feb. 1975, p. 27.

[15] Erdos, J. and Pallone, A., "Shock-Boundary Layer Interaction and Flow Separation," AVCO RAD-TR-61-23, Wilmington, Mass.,1961.

[16] Popinski, Z., and C. F. Ehrlich, "Development Design Methods for Predicting Hypersonic Aerodynamic Control Characteristics," AFFDL-TR-66-85, Air Force Flight Dynamics Lab., Wright-Patterson AFB, Ohio, Sept. 1966.

[17] Reshotko, E. and Tucker, M., "Effect of a Discontinuity on Turbulent Boundary-Layer Thickness Parameters with Application to Shock-Induced Separation," NACA TN-345, May 1955.

[18] White, R. A., "Turbulent Boundary Layer Separation from Smooth Convex Surfaces in Supersonic Two-Dimensional Flow," Ph.D. dissertation, Mechanical Engineering Dept., University of Illinois, Urbana, Ill., 1963.

[19] Kessler, T. J. and Page, R. H., "Supersonic Turbulent Boundary Layer Separation Ahead of a Wedge," *Developments in Mechanics*, Vol. 4, Aug. 1967, pp. 1011-1028.

[20] Batham, J. P., "A Reattachment Criterion for Turbulent Supersonic Flow," *AIAA Journal*, Vol. 7, July 1969, pp. 154-155.

[21] Pinckney, S. Z., "Semiempirical Method for Predicting Effects of Incident-Reflecting Shocks on the Turbulent Boundary Layer," NASA TN D-3029, Oct. 1965.

[22] Todisco, A. and Reeves, B. L., "Turbulent Boundary Layer Separation and Reattachment at Supersonic and Hypersonic Speeds," *Proceedings of the Symposium on Viscous Interaction Phenomena in supersonic and Hypersonic Flow*, USAF Aerospace Research Labs., Wright-Patterson AFB, Ohio, May 1969.

[23] Wilcox, D. C., "Numerical Study of Separated Turbulent Flows," ARL TR 74-0133, Aerospace Research Lab., Wright-Patterson AFB, Ohio, Nov. 1974.

[24] Shang, J. S. and Hankey, W. L., Jr., "Supersonic Turbulent Separated Flows Utilizing the Navier-Stokes Equations," AGARD-CPP-168: Flow Separation, May 1975.

[25] Havener, A. G. and Radley, R. J., "Supersonic Wind Tunnel Investigations Using Pulsed Laser Holography," ARL Rept. 73-0148, Aerospace Research Lab., Wright-Patterson AFB, Ohio, Oct. 1973.

[26] Horstman, C. C., Settles, G. S., Vas, I. E., Bogdonoff, S. M., and Hung, C. M., "Reynolds Number Effects on Shock-Wave Turbulent Boundary Layer Interactions – A Comparison of Numerical and Experimental Results," Paper to be presented at AIAA 15th Aerospace Sciences Meeting, Los Angeles, Calif., Jan. 24-16, 1977.